Kinematically complete experiment on transfer excitation in intermediate-energy $p+$He collisions

A. Hasan,[1,2] B. Tooke,[1] M. Zapukhlyak,[3] T. Kirchner,[3] and M. Schulz[1]
[1]*Physics Department and Laboratory for Atomic, Molecular, and Optical Research, University of Missouri-Rolla, Rolla, Missouri 65409, USA*
[2]*Department of Physics, UAE University, P.O. Box 17551, Alain, Abu Dhabi, United Arab Emirates*
[3]*Institut für Theoretische Physik, TU Clausthal, Leibnizstrasse 10, 38678 Clausthal-Zellerfeld, Germany*
(Received 19 June 2006; published 15 September 2006)

We have performed a kinematically complete experiment on transfer excitation in intermediate-energy proton-helium collisions. The differential cross sections were compared to double excitation data and a nonperturbative time-dependent calculation. This comparison reveals the importance of dynamic couplings between the motion of the heavy nuclei and electronic transitions and/or electron-electron correlation effects.

DOI: 10.1103/PhysRevA.74.032703 PACS number(s): 34.50.Fa, 34.50.Pi, 34.70.+e

INTRODUCTION

Atomic processes in which two (or more) electrons actively undergo a transition have been extensively studied ([1–3] and references therein) because the electron-electron interaction (in the following referred to as the ee interaction) tends to play a much more important role than in processes where only one electron undergoes a transition. The ee interaction, in turn, has attracted a lot of interest as it can lead to pronounced correlation effects. Unfortunately, it is usually very difficult to disentangle such effects from the dynamics of the two-center potential generated by the two nuclei. Therefore, in order to extract the maximum amount of information on correlation effects from the experimental data, kinematically complete experiments, i.e., experiments which determine the momentum vectors of all collision fragments, are crucially important.

For most two electron processes, investigators are faced with severe problems both in performing a kinematically complete experiment and the theoretical interpretation of the data. Although double ionization has been studied extensively (e.g., [4–10]), a major difficulty is that the final state involves four collision fragments so that (taking advantage of momentum conservation) three momentum vectors have to be measured directly. As a result, no fully differential cross sections (FDCS) on double ionization have been reported yet for ion impact and only one experiment got even close [10]. Only for electron impact, FDCS have become available in recent years [11–13]. Furthermore, the theoretical description of the FDCS is very difficult because the final state involves a two-electron continuum. As a result, satisfactory agreement with the experimental data has not been achieved yet.

Double excitation is kinematically simpler because the final state only contains three unbound particles (including the electron ejected by the autoionization of the doubly excited state). However, the identification of the process is more difficult involving either the detection of the autoionized electron in high resolution (e.g., [14]) (radiative decay is negligible) or a projectile energy-loss analysis [15,16]. A more serious problem arises in the interpretation of the data. Because the autoionization channel is indistinguishable from the direct ionization channel, the electron energy spectra exhibit pronounced interference effects, which are known as Fano interferences [17]. Here again, satisfactory agreement between experiment and theory has not been achieved yet.

An appealing alternative to study electron-electron correlation effects in atomic collisions is offered by transfer excitation (TE), i.e., the capture of one target electron with simultaneous excitation of the second electron. Kinematically, it is even simpler than double excitation since the final state only contains two unbound particles (the momentum of the photon emitted by the decay of the excited state is negligible). Furthermore, theory is not confronted with the above mentioned problems introduced by a many-electron continuum or by Fano interference. Finally, for proton-helium collisions the electronic final state is accurately known as for both collision partners the wave function is hydrogenic.

Surprisingly few studies have been performed on TE [much more work has been done on capture with simultaneous projectile excitation (e.g., [18–20])]. Total cross sections have been measured for multiply-charged ion impact (e.g., [21]) The only experimental study of differential TE cross sections was performed for slow protons colliding with heavy targets. However, there only $\Delta n=0$ excitation of the residual target ion was investigated [22]. Furthermore, in that experiment TE could not be fully distinguished from single ionization and the data had to be corrected for an estimated contribution from the latter process. For proton-helium collisions, the most simple system for which TE can occur, total cross sections have been measured for photon emission from He^+ ions [23,24], but in those experiments TE could not be distinguished from ionization plus excitation. To the best of our knowledge no measured total TE cross sections are available for $p+$He collisions and no differential cross sections for TE involving $\Delta n \neq 0$ for any collision system. In this paper we report the first measured differential cross sections for this process.

EXPERIMENT

The experiment was performed at the reaction microscope facility of the University of Missouri-Rolla. A proton beam was extracted with a 5 kV potential from a hot cathode ion source, accelerated to energies of 25, 50, and 75 keV and collimated by a set of slits 0.1×0.1 mm^2 in size located just

before the collision chamber. It was then crossed with a cold ($T<1$ K) neutral helium beam from a supersonic gas jet. The projectiles which were not neutralized in the collision were deflected out by a switching magnet and the neutralized projectiles were detected with a channel-plate detector.

The recoil-ions were extracted perpendicular to the incident projectile beam by a weak, nearly uniform electric field of 1.6 V/cm. After the electric field region, the recoil ions traveled through a field free region and were detected by a two-dimensional position-sensitive detector with a position resolution of ±50 μm. The recoil-ion detector was set in coincidence with the projectile detector. From the position information the y and z components of the recoil-ion momentum could be determined. The x component was obtained from the time of flight from the collision region to the detector, which, in turn, is obtained from the coincidence time spectrum. The achieved resolution is ±0.1 a.u. in the y direction (target beam direction) and ±0.075 a.u. in the x (perpendicular to target- and projectile beam directions), and z directions (projectile beam direction).

RESULTS AND DISCUSSION

For a process in which no electrons are ejected into the continuum, the longitudinal recoil-ion momentum p_{rz} (in a.u.) is related to the Q value (i.e., the difference between the initial and final total internal energy of the system) by $p_{rz}=-Q/v_0-nv_0/2$ [25], where v_0 is the projectile velocity and n is the number of captured electrons. Since the Q value has a well-defined value for a given process, p_{rz} is discrete for capture and excitation processes and can thus be used to identify them. Because of momentum conservation, the transverse recoil-ion momentum $p_{rt}=(p_{rx}{}^2+p_{ry}{}^2)^{1/2}$ has to be equal to the transverse final projectile momentum p_{pt}, which, in turn, is related to the scattering angle θ by $p_{pt}=p_0 \sin\theta$, where p_0 is the initial projectile momentum.

In Fig. 1 p_{rt} is plotted versus p_{rz} for 25 keV p+He on a logarithmic scale. In the longitudinal direction, the discrete lines separating the various processes are clearly visible. The dominant line at about 270 channels is due to capture to the ground state of the projectile and the line at about 300 channels represents capture to all higher projectile states. Finally, transfer excitation, the process we are mostly interested in, leads to the line at about 350 channels. The projection of each line onto the p_{rt} axis is proportional to the differential cross section $d\sigma/d\theta$ of the corresponding process. Absolute cross sections were obtained by normalizing the integrated counts in the capture lines to accurately known total capture cross sections [26]. The normalized cross sections were then converted to cross sections differential in the solid angle. To test the recoil-ion momentum calibration and the normalization we compared our differential capture cross sections to the data of Martin *et al.* [27] and found excellent agreement. The differential transfer excitation cross sections are shown in Fig. 2 for (from top to bottom) 25, 50, and 75 keV.

In the following we attempt to analyze to what extent the data can be explained without incorporating any electron-electron correlation effects. To this end, we performed calculations based on the independent particle model (IPM). The

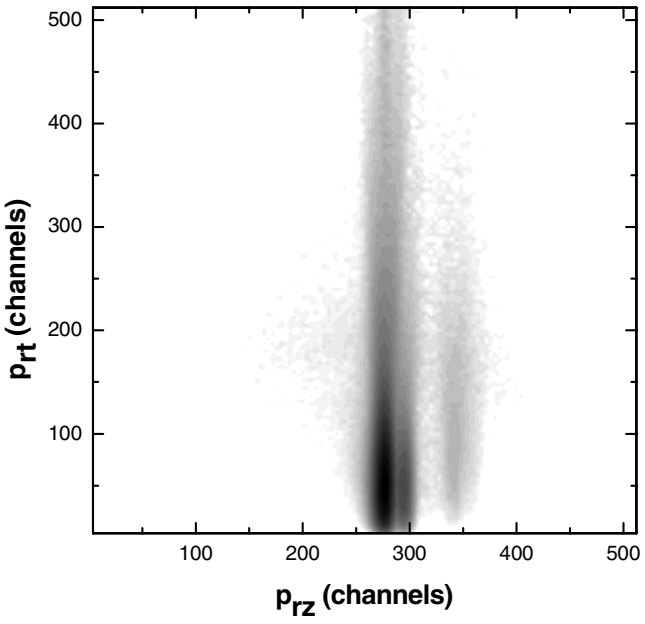

FIG. 1. Transverse versus longitudinal recoil-ion momentum distribution in 25 keV p+He collisions. The intensity is plotted on a logarithmic scale.

details of the theoretical method were reported previously [28,29] and only the salient points will be outlined here. We employ a semiclassical approximation, in which the motion of the nuclei is described in terms of straight-line trajectories. The electronic wave function is found from a solution of the time-dependent single-electron Schrödinger equation for a static Hartree-Fock potential using the basis generator method (BGM) [28]. We thus obtain single-electron transition probabilities $P[b(\Theta)]$ as a function of impact parameter b which corresponds classically to the scattering angle Θ (for simplicity, in the following we use $P(\Theta)$ as a short form for $P[b(\Theta)]$). The two-electron transition probabilities are then calculated using multinomial statistics [29]. The cross section differential in solid angle for any inelastic process $d\sigma_{\rm in}/d\Omega(\Theta)$ as a function of Θ is obtained using the ansatz of Greenland [30]

$$d\sigma_{\rm in}/d\Omega(\Theta) = d\sigma_{\rm el}/d\Omega(\Theta)P_x(\Theta), \tag{1}$$

where $d\sigma_{\rm el}/d\Omega(\Theta)$ is the cross section for classical elastic scattering from a potential $V(R)$ (R is the internuclear distance) and $P_x(\Theta)$ is the electronic transition probability for process x. Singly differential multiple ionization cross sections were calculated in a similar framework (e.g., [31]). For $V(R)$ we use the screened potential suggested by Greenland for capture processes [30]. The results of this calculation are shown as solid curves in Fig. 2.

Although, considering the difficulty in calculating cross sections for two-electron processes, the agreement with the data is not unreasonable, especially at the smallest projectile energy, significant discrepancies are quite apparent. In order to further analyze these discrepancies it is useful to compare the transfer-excitation to single capture cross section ratios

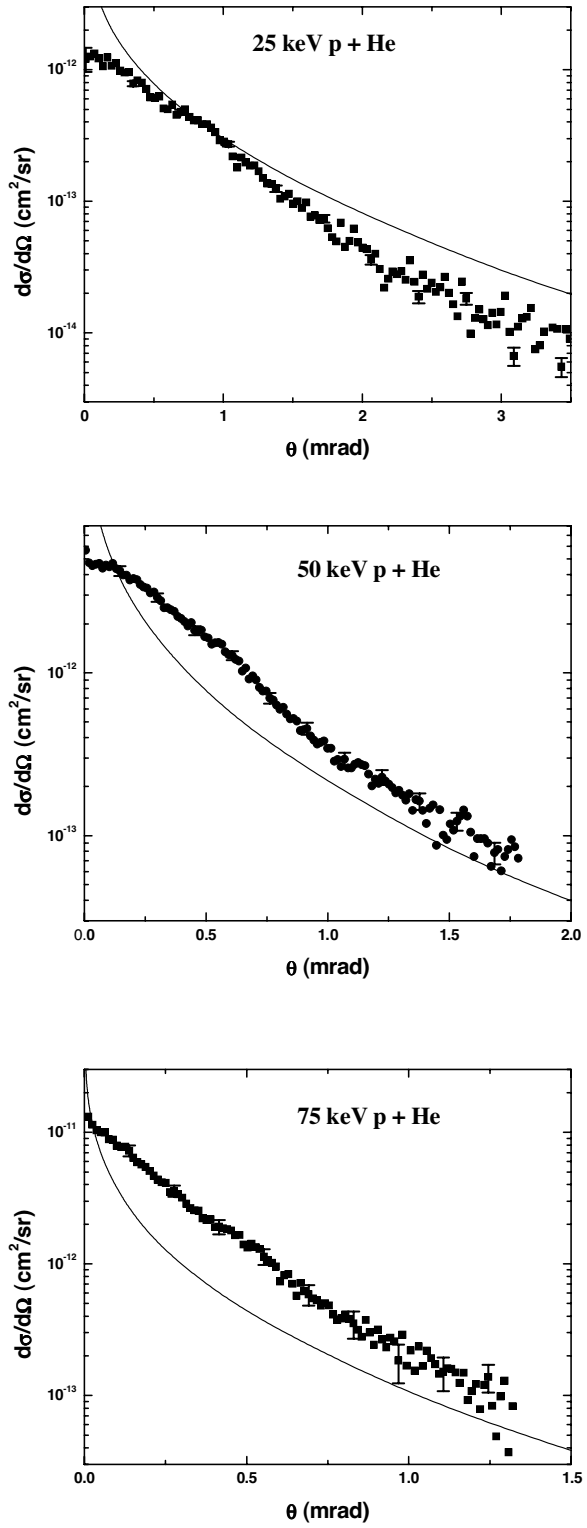

FIG. 2. Differential transfer-excitation cross sections as a function of scattering angle for 25, 50, and 75 keV p+He. The solid lines show nonperturbative time-dependent calculations based on the basis generator method.

$R_{TE}(\Theta)=[d\sigma_{TE}/d\Omega(\Theta)]/[d\sigma_{SC}/d\Omega(\Theta)]$ to the corresponding ratios $R_{DE}(\Theta)=[d\sigma_{DE}/d\Omega(\Theta)]/[d\sigma_{SE}/d\Omega(\Theta)]$ for double to single excitation. According to Eq. (1) the cross section ratios for two processes x and y can be written as

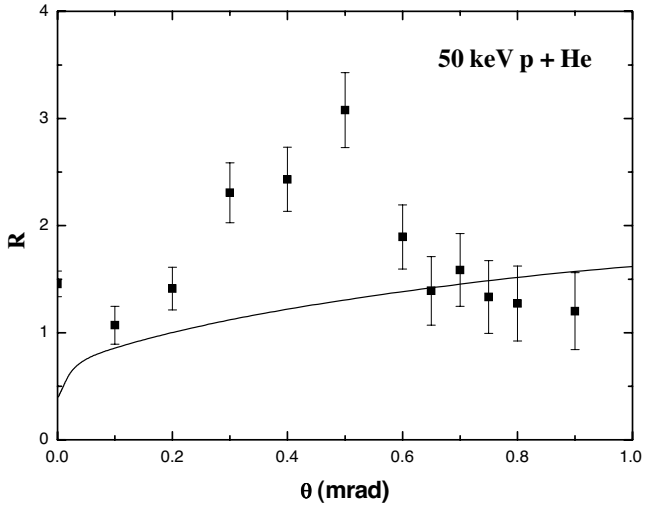

FIG. 3. Ratio between transfer-excitation to single capture and double to single excitation cross-section ratios as a function of scattering angle. Solid line as in Fig. 2, but different screenings were used for the various processes.

$$R_{xy}(\Theta)=[d\sigma_{el}^{x}/d\Omega(\Theta)P_x(\Theta)]/[d\sigma_{el}^{y}/d\Omega(\Theta)P_y(\Theta)], \quad (2)$$

where $d\sigma_{el}^{x}/d\Omega(\Theta)$ and $d\sigma_{el}^{y}/d\Omega(\Theta)$ are the classical cross sections for scattering from the potential $V(R)$ used in the calculations for both processes. If $V(R)$ is identical for both processes, Eq. (2) reduces to $R_{xy}(\Theta)=P_x(\Theta)/P_y(\Theta)$. Applying multinomial statistics to the transfer-excitation and double excitation probabilities, we then get

$$R_{TE}(\Theta)=2P_{SE}(\Theta)P_{SC}(\Theta)/[2P_{SC}(\Theta)P_{NT}(\Theta)], \quad (3a)$$

and

$$R_{DE}(\Theta)=P_{SE}(\Theta)^2/[2P_{SE}(\Theta)P_{NT}(\Theta)], \quad (3b)$$

or

$$R(\Theta)=R_{TE}(\Theta)/R_{DE}(\Theta)=2, \quad (3c)$$

where $P_{SE}(\Theta)$, $P_{SC}(\Theta)$, and $P_{NT}(\Theta)$ are the single electron probabilities for excitation, capture, and no electronic transition at all, respectively.

In Fig. 3 the measured ratios $R(\Theta)$ are plotted for a projectile energy of 50 keV, where the experimental data for $R_{DE}(\Theta)$ were taken from Schulz *et al.* [16]. For 25 and 75 keV measured data for $R_{DE}(\Theta)$ are not available. Quite obviously, the experimental $R(\Theta)$ are not constant at 2. On the other hand, it is not realistic to assume that $V(R)$ is identical for all processes, since an electronic transition leads to a change of the screening of the scattering potential. This change in screening is generally not the same for different processes. For example, in a capture process the initially unscreened proton-projectile becomes fully screened at large distances while the screening of the target nucleus is reduced. On the other hand, in an excitation process only the screening of the target matters. We therefore used different screening functions for $V(R)$ in our calculation of $R(\Theta)$: For transfer excitation and single capture we used Greenland's potential [30], while for single and double excitation we used

a similarly constructed potential that accounts for the screening of the He nucleus by two electrons. The results are shown as the solid line in Fig. 3. Indeed, in this model $R(\Theta)$ is no longer constant and reaches a value of 2 only asymptotically for large Θ. Nevertheless, satisfactory agreement with the data is only achieved for scattering angles larger than 0.6 mrad. The maximum in the measured values at about 0.5 mrad is not reproduced by the calculation.

The theoretical model contains four potentially far-reaching approximations, which are thus prime candidates for causing the discrepancies between theory and experiment: (a) Electron-electron correlations are not included. (b) Although couplings between the nuclei and the electrons are partially accounted for by using different screenings for different processes, dynamic couplings are not included because the screening is not time-dependent. (c) Deflection of the projectile off the electrons is only accounted for in terms of the screening, but incoherent deflection from an electronic scattering center is not included. (d) Equation (1), which describes the inelastic cross sections in terms of classical elastic scattering, is not valid for small scattering angles [30].

Maxima around 0.5 mrad have also been observed in, e.g., transfer ionization (TI) to single ionization cross section ratios $R_{\mathrm{TI}}(\Theta)$. They were explained in terms of the so called Thomas process of the second kind ($T2$), which involves both incoherent projectile-electron scattering and electron-electron correlations [32]. The same process could potentially also contribute to TE and lead to structures at the same scattering angle as in TI. In TI, the maxima occurred only at projectile energies larger than approximately 150 keV [33]. However, it should be noted that the ratio $R(\Theta)$ is much more sensitive to the $T2$ process than $R_{\mathrm{TE}}(\Theta)$ and $R_{\mathrm{TI}}(\Theta)$ because it is basically a direct measure of all factors leading to a deviation from Eq. (1) or from multinomial statistics for the electron transition probabilities, such as the $T2$ mechanism. Therefore, we do not rule out the possibility that the peak in $R(\Theta)$, occurring at the angle expected for the $T2$ process, is indeed due to this mechanism. However, we also note that in the case of TI this explanation has been disputed [34].

Dynamic nucleus-electron couplings may also contribute to the discrepancies between experiment and theory. They are likely to mainly affect small scattering angles because increasing angles favor increasingly closer collisions where the screening becomes less important. Indeed, the agreement between experiment and theory seems to be better at large angles. However, it is not clear how accurate the calculation is at small scattering angles because we do not have enough data in that region. It is quite possible that the discrepancies mainly comprise the nonreproduction of the peak at intermediate angles. Finally, according to Eq. (20) of Greenland [30], Eq. (1) may not be valid for angles smaller than about 0.5 mrad for our collision system. However, empirically it was found that Eq. (1) holds at much smaller angles than suggested by the condition of Greenland [35].

CONCLUSIONS

We have measured differential transfer-excitation cross sections. A comparison to double excitation data and to our nonperturbative time-dependent calculations shows that the experimental findings cannot be explained in terms of an independent particle model. The discrepancies between experiment and theory can be traced to dynamic nucleus-electron couplings and/or electron-electron correlation effects. The latter possibly manifests itself in terms of a Thomas peak at 0.5 mrad in $R(\Theta)$. As a next step, we plan to perform calculations on the time-dependent Hartree-Fock level for the electronic wave function, and possibly also with time-dependent scattering potentials. Such a calculation appears to be feasible, but presents a tedious and time-consuming challenge. The ultimate goal is to transcend the classical approximation (1) and to also incorporate electron-electron correlations in the theoretical model.

ACKNOWLEDGMENT

This work was supported by the National Science Foundation under Grant No. PHY-0353532.

[1] J. Berakdar, A. Lahmam-Bennani, and C. Dal Cappello, Phys. Rep. **374**, 91 (2003).
[2] M. Schulz, Int. J. Mod. Phys. B **9**, 3269 (1995).
[3] J. Ullrich, R. Moshammer, A. Dorn, R. Dörner, L. P. H. Schmidt, and H. Schmidt-Böcking, Rep. Prog. Phys. **66**, 1463 (2003).
[4] L. H. Andersen, P. Hvelplund, H. Knudsen, S. P. Møller, K. Elsener, K.-G. Rensfelt, and E. Uggerhøj, Phys. Rev. Lett. **57**, 2147 (1986).
[5] J. P. Giese and E. Horsdal, Phys. Rev. Lett. **60**, 2018 (1988).
[6] B. Skogvall and G. Schiewietz, Phys. Rev. Lett. **65**, 3265 (1990).
[7] R. Moshammer, J. Ullrich, H. Kollmus, W. Schmitt, M. Unverzagt, O. Jagutzki, V. Mergel, H. Schmidt-Böcking, R. Mann, C. J. Woods, and R. E. Olson, Phys. Rev. Lett. **77**, 1242 (1996).
[8] B. Bapat, S. Keller, R. Moshammer, R. Mann, and J. Ullrich, J. Phys. B **33**, 1437 (2000).
[9] M. Schulz, R. Moshammer, W. Schmitt, B. Feuerstein, H. Kollmus, R. Mann, S. Hagmann, and J. Ullrich, Phys. Rev. Lett. **84**, 863 (2000).
[10] D. Fischer, R. Moshammer, A. Dorn, J. R. Crespo López-Urrutia, B. Feuerstein, C. Höhr, C. D. Schröter, S. Hagmann, H. Kollmus, R. Mann, B. Bapat, and J. Ullrich, Phys. Rev. Lett. **90**, 243201 (2003).
[11] I. Taouil, A. Lahmam-Bennani, A. Duguet, and L. Avaldi, Phys. Rev. Lett. **81**, 4600 (1998).
[12] A. Dorn, A. Kheifets, C. D. Schröter, B. Najjari, C. Höhr, R. Moshammer, and J. Ullrich, Phys. Rev. Lett. **86**, 3755 (2001).
[13] A. Dorn, A. Kheifets, C. D. Schröter, C. Höhr, G. Sakhelashvili, R. Moshammer, J. Lower, and J. Ullrich, Phys. Rev. A **68**, 012715 (2003).

[14] J. P. Giese, M. Schulz, J. K. Swenson, H. Schöne, M. Benhenni, S. L. Varghese, R. Vane, P. F. Dittner, M. Benhenni, S. M. Shafroth, and S. Datz, Phys. Rev. A **42**, 1231 (1990).
[15] W. T. Htwe, T. Vajnai, M. Barnhart, A. D. Gaus, and M. Schulz, Phys. Rev. Lett. **73**, 1348 (1994).
[16] M. Schulz, W. T. Htwe, A. D. Gaus, J. L. Peacher, and T. Vajnai, Phys. Rev. A **51**, 2140 (1995).
[17] U. Fano, Phys. Rev. **124**, 1866 (1961).
[18] J. A. Tanis, E. M. Bernstein, W. G. Graham, M. P. Stockli, M. Clark, R. H. McFarland, T. J. Morgan, K. H. Berkner, A. S. Schlachter, and J. W. Stearns, Phys. Rev. Lett. **53**, 2551 (1984).
[19] M. Schulz, E. Justiniano, R. Schuch, P. H. Mokler, and S. Reusch, Phys. Rev. Lett. **58**, 1734 (1987).
[20] E. Y. Kamber, M. A. Abdallah, C. L. Cocke, M. Stöckli, J. Wang, and J. P. Hansen, J. Phys. B **33**, L171 (2000).
[21] H. Cederquist, Phys. Rev. A **43**, 2306 (1991).
[22] S. Knoop, R. Morgenstern, and R. Hoekstra, Phys. Rev. A **70**, 050702(R) (2004).
[23] K.-H. Schartner, B. Lommel, and D. Detleffsen, J. Phys. B **24**, L13 (1991).
[24] W. C. Stolte and R. Bruch, Phys. Rev. A **54**, 2116 (1996).
[25] J. Ullrich, R. Moshammer, R. Dörner, O. Jagutzki, V. Mergel, H. Schmidt-Böcking, and L. Spielberger, J. Phys. B **30**, 2917 (1997).
[26] Atomic Data for Fusion, http://www-cfadc.phy.ornl.gov/redbooks/redbooks.html.
[27] P. J. Martin, D. M. Blankenship, T. J. Kvale, E. Redd, J. L. Peacher, and J. T. Park, Phys. Rev. A **23**, 3357 (1981).
[28] O. J. Kroneisen, H. J. Lüdde, T. Kirchner, and R. M. Dreizler, J. Phys. A **32**, 2141 (1999).
[29] T. Kirchner, L. Gulyás, H. J. Lüdde, E. Engel, and R. M. Dreizler, Phys. Rev. A **58**, 2063 (1998).
[30] P. T. Greenland, J. Phys. B **14**, 3707 (1981).
[31] J. Ullrich, M. Horbatsch, V. Dangendorf, S. Kelbch, and H. Schmidt-Böcking, J. Phys. B **21**, 611 (1988).
[32] E. Horsdal, B. Jensen, and K. O. Nielsen, Phys. Rev. Lett. **57**, 1414 (1986).
[33] S. W. Bross, S. M. Bonham, A. D. Gaus, J. L. Peacher, T. Vajnai, M. Schulz, and H. Schmidt-Böcking, Phys. Rev. A **50**, 337 (1994).
[34] R. Gayet and A. Salin, Nucl. Instrum. Methods Phys. Res. B **56**, 82 (1991).
[35] M. Horbatsch, J. Phys. B **22**, L639 (1989).